Proc. of the European Safety and Reliability Conference (ESREL 2026)
Edited by José C. Matos, Paulo B. Lourenço, Michael Beer, Daniel Oliveira,
Edoardo Patelli, Hélder S. Sousa, Rui A. Silva and Monica Santamaria

doi: 10.3850/ESREL2026061419_esrel26-p27679-cd

Probabilistic System-Level Prognostics for Reliability and Risk Assessment in Aerospace Structures

Mariana Salinas-Camus
E-mail: *m.salinascamus@tudelft.nl*

Oscar Carpentier

Nick Eleftheroglou
E-mail: *n.eleftheroglou@tudelft.nl*

Intelligent System Prognostics, Faculty of Aerospace Engineering, Delft University of Technology, Kluyverweg 1, Delft, 2629 HS, Netherlands.

System-Level Prognostics (SLP) is essential for ensuring mission success, as it focuses on predicting the System Remaining Useful Life (SRUL) rather than individual subsystem RULs. Unlike subsystem-level prognostics, SLP must account for degradation interactions and quantify inherent uncertainty. In aerospace structures, however, system-scale failure data are scarce due to cost and safety constraints, limiting the applicability of existing methods. This paper introduces the RUL Inoperabilities Model (RIM), a probabilistic framework inspired by the Inoperability Input–Output Model (IIM) that operates directly on coupon-level RUL predictions. The approach is prognostic model-agnostic, interpretable, and data-efficient, requiring only coupon-level training data and a single component-level degradation history to capture interdependencies. RIM propagates probabilistic coupon-level predictions to the component level, providing uncertainty-aware SRUL estimates without additional full-scale testing.
The framework is validated using a component composed of three interconnected open-hole aluminum coupons, with a Hidden Semi-Markov Model (HSMM) used as the base predictor. Results show that RIM improves SRUL accuracy and uncertainty calibration compared to a naive aggregation approach. Beyond RUL-prognostics, the probabilistic SRUL outputs are used to perform conditional reliability and risk-based working subsystem analyses, enabling assessment of both remaining life and functional degradation. Overall, RIM provides a scalable and reliability-informed solution for system-level prognostics under limited data in the scale of interest.

Keywords: system-level prognostics, remaining useful life, uncertainty quantification, reliability, risk assessment.

1. Introduction

Prognostics provide critical information for operational decision-making and mission success Elattar et al. (2016). To ensure a mission is completed safely and effectively, the entire system must perform reliably, making system-level prognostics (SLP) essential. Unlike component-level approaches, SLP aims to predict the Remaining Useful Life (RUL) of the complete system. Equally important is that the SRUL is a random variable rather than a deterministic quantity Salinas-Camus et al. (2025). At the system level, inaccurate prediction of the system RUL (SRUL) can lead to premature mission termination or unexpected failures, with significant operational and safety implications.

In aerospace applications, the emphasis shifts from generic systems to structures. Structures connect all subsystems and often govern mission continuation. However, collecting structure-level failure data is rarely feasible due to cost and safety constraints. For instance, civil aircraft certification typically relies on only two full-scale structural tests: one quasi-static and one fatigue test. This scarcity of data motivates the development of methods that can be trained using lower-scale experiments, such as coupon or element tests, while still providing accurate and uncertainty-aware SRUL predictions.

Most Prognostics and Health Management

(PHM) methods are developed at small scales, such as composite coupons, which limits their direct applicability to full aerospace structures Broer et al. (2022). The building block approach addresses this limitation by validating models at progressively larger scales, from coupons to full structures. For consistency with structural terminology, this paper uses coupon to denote a subsystem and component to denote the overall system.

Many existing SLP methods model a component either as a collection of independent coupons or as a black box driven by input–output data Tamssaouet et al. (2023). While computationally efficient, these approaches often require large datasets and fail to capture interdependencies among coupons. More advanced methods incorporate such interactions using physics-based models Khorasgani et al. (2016), ensemble learning Galanopoulos et al. (2023), particle filtering Rodrigues (2018); Khorasgani et al. (2016), agent-based modeling Benaggoune et al. (2018), or graph convolutional networks Palazuelos and Droguett (2021). Although powerful, these techniques are frequently computationally intensive, data-hungry, and difficult to interpret.

The Inoperability Input–Output Model (IIM), originally developed in economics Leontief (1936) and later adapted to engineering systems Tamssaouet et al. (2021, 2018), offers a more interpretable alternative for modeling interdependencies. However, its application to aerospace SLP is limited by its reliance on physics-based degradation models and not propagating uncertainty from coupon-level predictions to SRUL.

To address these limitations, this paper introduces the RUL Inoperabilities Model (RIM), a probabilistic framework inspired by the IIM that operates directly on coupon-level RUL predictions. RIM is prognostic model-agnostic and does not require predefined interaction mechanisms between coupons. It extends the IIM by propagating probabilistic coupon-level predictions to obtain a probabilistic SRUL. The method requires only coupon-level training data and can adapt online as system behavior evolves. The resulting probabilistic SRUL enables conditional reliability analysis and risk assessment, which are critical for aerospace structures.

The proposed approach is validated through real data extracted from a conceptual aerospace structure case study involving non-linear interactions between coupons, using open-hole aluminum specimens as the basis for coupon-level prognostic models. The results show that RIM effectively propagates uncertainty from coupon-level RUL predictions to component-level SRUL, enabling reliable system-level prognostics despite limited component-scale data.

2. Methodology

The RUL Inoperabilities Model (RIM) framework and its training methodology are presented in subsection 2.1. An overview of the complete system-level prognostics (SLP) pipeline, from coupon-level condition monitoring (CM) data to system-level RUL (SRUL) prediction, is shown in Figure 1. Coupon CM data are processed by base prognostic models to produce coupon-level RUL predictions. These predictions are then transformed by the RIM to account for interdependencies among coupons, yielding adapted RULs. Finally, the SRUL is obtained by aggregating the adapted RULs using an operator $f(\cdot)$ selected to reflect the component behavior (e.g., minimum, maximum, or mean).

2.1. *RUL Inoperabilities Model (RIM)*

The RIM operates in two stages: an *offline* training phase and an *online* testing phase. A schematic overview of the process is shown in Figure 2.

During the offline phase, base prognostic models are applied to coupon-level data to estimate the vector of coupon RUL predictions, denoted as $\mathrm{RUL}_C(t)$. These predictions, together with an initial estimate of the interdependency matrix A_{init}, are used to construct the initial RIM model. The matrix A_{offline} is learned using a training dataset composed of coupon-level RUL predictions obtained when independently trained base predictors are applied to full-component data.

It is important to note that the base predictors are trained exclusively on coupon data and are not exposed to component-level data during training. Consequently, the offline training dataset captures

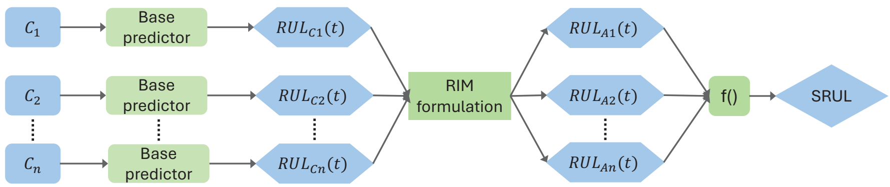

Fig. 1.: General framework of the proposed RIM for SRUL predictions.

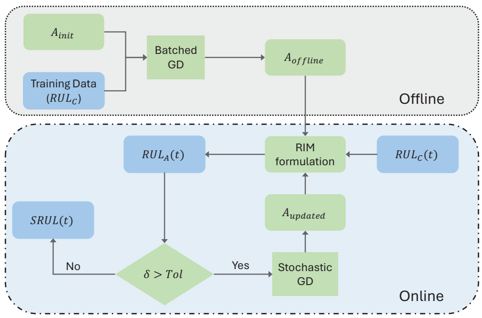

Fig. 2.: Flowchart of the adapted RIM's online and offline workings.

the collective behavior of independent coupon-level models when deployed at the component scale.

In the online phase, the RIM operates in real time by receiving updated coupon-level RUL predictions, $\mathrm{RUL}_C(t)$. These predictions are transformed into adapted RULs, denoted as $\mathrm{RUL}_A(t)$, through the interdependency matrix A. The matrix A is adaptively updated during operation to reflect changes in component behavior. The SRUL is then computed by applying an aggregation operator $f(\cdot)$ to the adapted RUL vector.

2.1.1. *Mathematical Formulation*

The original Inoperability Input–Output Model (IIM) Tamssaouet et al. (2018) is expressed as:

$$q(t) = A \cdot q(t-1) + c(t), \tag{1}$$

where $q(t)$ represents the vector of system inoperabilities. For application to structural prognostics, the RIM departs from the original formulation by operating directly on predicted RULs and omitting explicit environmental effects.

Structural degradation is inherently coupled, as the condition of one coupon may influence the degradation of others. To capture these interactions, the RIM introduces a relative degradation vector $z(t)$, allowing interdependencies to be modeled implicitly through the matrix A. The RIM formulation is given by:

$$\mathrm{RUL}_A(t) = \mathrm{RUL}_C(t) \circ (A \cdot z(t)) + \mathrm{RUL}_C(t), \tag{2}$$

where $\circ$ denotes the Hadamard product. The relative degradation vector is defined as:

$$z(t) = \frac{\mathrm{RUL}_C(t)}{\mathrm{mean}(\mathrm{RUL}_C(t))}, \tag{3}$$

which represents the degradation of each coupon relative to the component average.

After computing the adapted coupon-level RULs, the SRUL at time t is obtained by aggregating $\mathrm{RUL}_A(t)$:

$$SRUL(t) = f\left(\mathrm{RUL}_A(t)\right), \tag{4}$$

where $f(\cdot)$ is selected to reflect the component failure behavior.

2.1.2. *Gradient Descent for Matrix Training*

The interdependency matrix A is the only trainable parameter of the RIM and is estimated using gradient descent during both offline and online phases. The model is trained by minimizing the Mean Squared Error (MSE) between the adapted RUL predictions and the true RUL values:

$$\mathcal{L}(\mathrm{RUL}_A, \mathrm{RUL}_{\mathrm{true}}) = \frac{1}{N} \cdot \sum_{i=1}^{N} \Big(\mathrm{RUL}_A^{(i)} - \mathrm{RUL}_{\mathrm{true}}^{(i)}\Big)^2. \tag{5}$$

The gradient of the loss with respect to each matrix entry a_{ij} is given by:

$$\frac{\partial \mathcal{L}}{\partial a_{ij}} = \frac{2}{N} \cdot \mathrm{RUL}_C^{(i)} \cdot \left(\mathrm{RUL}_A^{(i)} - \mathrm{RUL}_{\text{true}}^{(i)} \right) \cdot z^{(j)}. \tag{6}$$

The matrix is updated according to:

$$a_{ij}^{\text{new}} = a_{ij}^{\text{prev}} - \lambda \cdot \frac{\partial \mathcal{L}}{\partial a_{ij}}, \tag{7}$$

where λ denotes the learning rate.

2.1.3. *Uncertainty Quantification in RIM*

Uncertainty quantification is essential in prognostics, as point estimates of RUL are insufficient for reliable decision-making Salinas-Camus et al. (2025). In the RIM framework, uncertainty at the coupon level is propagated to the SRUL through a sampling-based approach.

At each time step, M samples are drawn from the probability distributions provided by the coupon-level base predictors. A stratified sampling strategy Shields et al. (2015) is used to ensure adequate coverage of the distributions while controlling computational cost. Each sample contains one RUL realization per coupon and is propagated through the RIM using Equation 2. The corresponding SRUL is then computed using Equation 4.

Repeating this procedure yields an empirical probability distribution of the SRUL at time t, providing both a mean estimate and confidence intervals. This process propagates only the uncertainty encoded in the coupon-level RUL predictions; uncertainty associated with the learned interdependency matrix A is not explicitly modeled.

2.2. *Conditional Reliability and Risk-Based Analysis*

The probabilistic SRUL predictions produced by the RIM enable further prognostic analyses that support reliability- and risk-informed decision-making. In this work, conditional reliability and risk are derived directly from the empirical SRUL distributions, without introducing additional degradation models or assumptions.

2.2.1. *Conditional Reliability*

Conditional reliability is defined as the probability that the component remains operational beyond a future time horizon τ, conditioned on the information available at time t. Let $\mathrm{SRUL}(t)$ denote the random variable representing the system-level RUL at time t Salinas-Camus et al. (2025). The conditional reliability is given by:

$$R(t + \tau \mid t) = \mathbb{P}\left(\mathrm{SRUL}(t) > \tau\right). \tag{8}$$

Using the sampling-based uncertainty propagation described in Section 2.1.3, this probability is estimated empirically from M SRUL samples:

$$R(t + \tau \mid t) = \frac{1}{M} \sum_{m=1}^{M} \mathbb{I}\left(\mathrm{SRUL}^{(m)}(t) > \tau \right), \tag{9}$$

where $\mathbb{I}(\cdot)$ denotes the indicator function. Evaluating this expression over a range of τ yields the conditional reliability curve at time t.

2.2.2. *Probability of Failure-based Risk Assessment*

Traditionally, failure in aerospace structures is defined by physical limit states, such as structural collapse or breakdown Zio and Pedroni (2012). However, relying on these binary physical definitions is often impractical for real-time operations, as it can lead to unnecessarily stringent regulatory burdens and excessive conservatism in design. To address this, modern safety engineering advocates for a transition toward Condition-Based Risk Assessment (CB-RA) Zio (2025). By using real-time monitoring data, reliability assessments can be dynamically updated to capture the specificity of individual equipment rather than relying on population averages.

Within this framework, risk is evaluated by comparing the current health state against predefined numerical safety or acceptance criteria. In this study, failure is redefined as the point at which the probability of failure for a future horizon τ exceeds a specified threshold, P_{fth} Gerrard and Tsanakas (2011). This approach treats the probability of failure as a risk metric to inform operational decisions regarding maintenance or mission continuation. Formally, the risk at time t for a horizon τ is expressed as:

$$P_f(t+\tau \mid t) = \mathbb{P}(\mathrm{SRUL}(t) \leq \tau) = 1-R(t+\tau \mid t). \tag{10}$$

By evaluating these curves against P_{fth}, the specific time each subsystem is considered "functionally failed" can be identified. This enables a dynamic assessment of functional degradation, allowing operators to monitor the remaining structural redundancy and resilience as the system evolves.

3. Case Study

The proposed RUL Inoperabilities Model (RIM) is evaluated using a conceptual aerospace aluminum component composed of three interconnected rectangular open-hole coupons. Coupon-level CM data from constant-amplitude fatigue tests (Figure 3a) are used to train the base prognostic model. The RIM is subsequently trained using strain data from only one multi-coupon component subjected to constant-amplitude fatigue loading (Figure 3b).

To evaluate the ability of the RIM to predict SRUL from coupon-level information, the framework is tested on four additional components subjected to fatigue loading under conditions similar to the single-coupon tests. The same type of CM data, i.e. axial strains, is collected during operation (an example is shown in Figure 3c).

3.1. *Coupon-level results with base predictor*

The base prognostic model is trained using CM data from single open-hole coupons. As discussed earlier, the RIM is compatible with any prognostic model capable of producing probabilistic RUL estimates. In this study, a Hidden Semi-Markov Model (HSMM) is adopted as the base predictor due to its stochastic formulation, unsupervised nature, and established effectiveness in degradation modeling Salinas-Camus et al. (2025); Loutas et al. (2022); Eleftheroglou et al. (2019). The HSMM prognostic implementation used in this work is available through the open-source HiMAP package Kontogiannis et al. (2026).

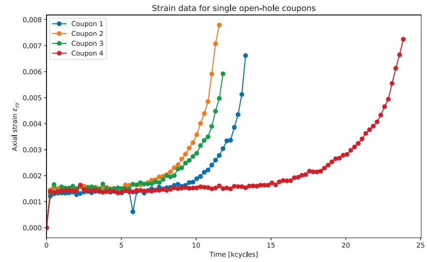

(a) Single open-hole coupons for base predictor training.

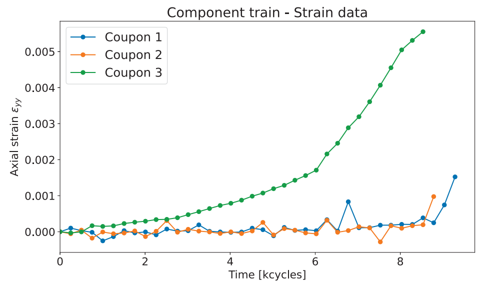

(b) Training component.

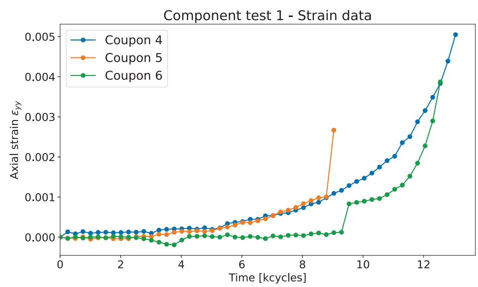

(c) Test component 1.

Fig. 3.: Raw strain-field data used for training and testing.

The base predictor provides smooth and stable coupon-level RUL trajectories while quantifying aleatoric uncertainty. Across 15 coupons from five components, the average coupon-level RMSE is 7.5 kcycles, indicating reliable baseline performance for subsequent system-level aggregation.

3.2. *RIM SRUL results*

With the coupon-level base predictor established, the RIM's ability to adapt coupon-level RUL predictions into system-level RUL (SRUL) predictions is evaluated. The base predictor trained on single-coupon data is used consistently across all components.

For offline training of the RIM, data from one multi-coupon component are used, while the remaining four components are reserved for testing. This setup reflects realistic aerospace scenarios, where only a limited number of component-level tests are typically available due to cost and experimental constraints.

Within the RIM framework, the aggregation operator $f(\cdot)$ is selected as the $\max(\cdot)$ operator, corresponding to a parallel component configuration in which system failure occurs when the last coupon fails.

As a baseline, a "Naive System RUL" (Naive SRUL) approach is implemented, in which the SRUL is computed directly as the maximum of the coupon-level RUL predictions at each time step. While intuitive, this approach neglects interactions among coupons and serves as a reference for evaluating the benefits of the RIM.

Performance is assessed using the Root Mean Squared Error (RMSE) and the Continuous Ranked Probability Score (CRPS) Hersbach (2000). Since CRPS accounts for both predictive accuracy and uncertainty calibration, it provides a comprehensive metric for probabilistic SRUL prediction Aizpurua et al. (2022).

The RIM hyperparameters used during the offline and online phases are summarized in Table 1. The parameter k is set to 3, as larger values reduce accuracy by overemphasizing past predictions, while the learning rate is chosen to ensure stable convergence. A comparison between the

Type	Learning rate	Iterations	Batch	k
Offline	1e-7	2000	True	–
Online	1e-5	100	True	3

Table 1.: Hyperparameters for the offline and online phases of the RIM.

RIM and the Naive SRUL approach across the four test components demonstrates consistent performance improvements. The mean SRUL-RMSE decreases from 7.58 to 6.82 kcycles.

More notably, the mean SRUL-CRPS decreases from 6.75 to 4.52, indicating that the RIM not only improves point prediction accuracy but also produces better-calibrated probabilistic SRUL estimates by explicitly accounting for coupon interdependencies.

Table 2.: SRUL RMSE and CRPS for baseline (Naive SRUL) and RIM across four test components.

Comp.	**SRUL-RMSE** [kcycles]		**SRUL-CRPS**	
	Baseline	**RIM**	**Baseline**	**RIM**
1	5.56	**5.45**	4.97	**4.94**
2	8.69	**7.87**	8.19	**3.39**
3	9.94	**7.84**	8.18	**4.76**
4	6.15	**6.13**	5.65	**4.98**
Mean	7.58	**6.82**	6.75	**4.52**

3.3. *Conditional Reliability and Risk-Based Working Subsystem Results*

While SRUL predictions provide valuable prognostic insight, operational decision-making often requires information expressed in terms of reliability and functional risk. For this reason, the probabilistic SRUL and adapted coupon-level RUL outputs produced by the RIM are further exploited to perform conditional reliability and risk-based working coupon analyses.

Conditional reliability quantifies the probability that the component will remain operational beyond a given future horizon, conditioned on the information available at a specific time, as described in subsection 2.2. Using the empirical SRUL distributions generated by the RIM, conditional reliability curves are computed at three inspection times using Equation 9.

Figure 4 shows the conditional reliability for Component 2. The dot indicates the mean predicted SRUL, while the vertical line represents the true SRUL; ideally, these should intersect, indicating accurate prediction. The figure illustrates both the evolution of conditional reliability at different inspection times and its relationship with SRUL predictions. As the conditioning time increases, reliability decays more rapidly, reflecting accumulated damage and reduced uncertainty as failure approaches.

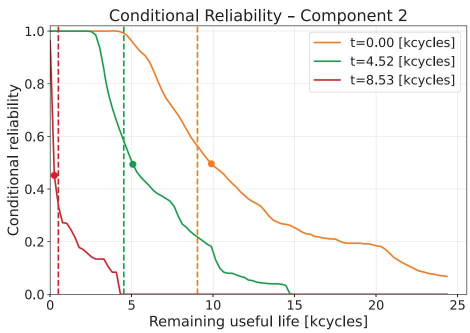

Fig. 4.: Conditional reliability at three different time steps for Component 2 using the RIM.

In addition to reliability, a risk-based working coupon (subsystem) analysis is conducted to assess the remaining functional capacity of the component, as defined in subsection 2.2.2. A coupon is considered failed when its probability of failure exceeds a predefined threshold, which is set to $P_f = 0.1$ for this case study. This threshold is selected for illustrative purposes; in practice, its value depends on the criticality of the structure and the nature of the associated risk, such as maintenance cost, loss of functionality, or safety considerations.

This analysis estimates the expected number of operational coupons over time since it can be used as a proxy for remaining structural functionality and redundancy. Figure 5 shows the evolution of the working subsystem for Component 2, comparing results obtained using the base predictor and the adapted RIM predictions.

The RIM-based results exhibit a more conservative reduction in the number of working coupons compared to the base predictor. From a risk perspective, this behavior is desirable for aerospace structures, as it provides a more realistic representation of functional degradation and enables the identification of operating regimes in

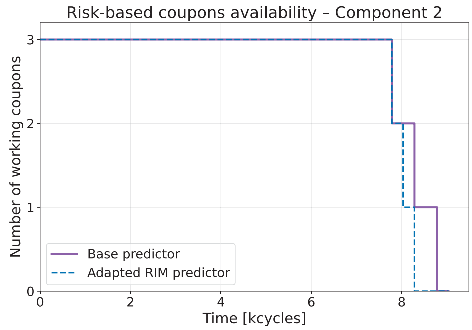

Fig. 5.: Risk-based analysis of coupon availability for Component 2.

which the component remains functional but with reduced redundancy.

Overall, these results demonstrate that the RIM framework extends prognostic outputs into reliability- and risk-informed indicators. By linking probabilistic SRUL predictions to conditional reliability and working subsystem metrics, the RIM supports decision-making processes that require both life prediction and assessment of functional degradation.

4. Conclusions

This paper introduces the RUL Inoperabilities Model (RIM), a probabilistic framework inspired by the Inoperability Input–Output Model (IIM) that operates directly on coupon-level RUL predictions. The approach is model-agnostic, interpretable, and data-efficient, requiring only coupon-level training data and a single component-level degradation history for adaptation. By propagating uncertainty from the coupon level to the component level, the RIM provides both SRUL point estimates and well-calibrated confidence bounds, which are essential for decision-making in aerospace applications.

The methodology was validated using single open-hole aluminum coupon experiments, with a Hidden Semi-Markov Model (HSMM) employed as the base predictor. The RIM consistently improved performance relative to a Naive SRUL baseline, achieving lower prediction errors and significantly reduced CRPS values, indicating more accurate and better-calibrated probabilistic predictions.

Beyond prognostics, the probabilistic SRUL outputs were further exploited to perform conditional reliability and risk-based working subsystem analyses. These results demonstrate that the RIM enables the translation of RUL predictions into reliability- and risk-informed indicators, supporting operational decisions that require both life estimation and assessment of functional degradation.

References

Aizpurua, J., B. Stewart, S. McArthur, M. Penalba, M. Barrenetxea, E. Muxika, and J. Ringwood (2022). Probabilistic forecasting informed failure prognostics framework for improved rul prediction under uncertainty: A transformer case study. *Reliability Engineering & System Safety 226*, 108676.

Benaggoune, K., H. Mouss, A. A. Abdessemed, and M. Bensakhria (2018). Agent-based prognostic function for multicomponents system with stochastic dependence. In *2018 International Conference on Applied Smart Systems (ICASS)*, pp. 1–5.

Broer, A. A. R., R. Benedictus, and D. Zarouchas (2022). The need for multi-sensor data fusion in structural health monitoring of composite aircraft structures. *Aerospace 9*(4).

Elattar, H. M., H. K. Elminir, and A. M. Riad (2016). Prognostics: a literature review. *Complex & Intelligent Systems 2*(2), 125–154.

Eleftheroglou, N., S. S. Mansouri, T. Loutas, P. Karvelis, G. Georgoulas, G. Nikolakopoulos, and D. Zarouchas (2019). Intelligent data-driven prognostic methodologies for the real-time remaining useful life until the end-of-discharge estimation of the lithium-polymer batteries of unmanned aerial vehicles with uncertainty quantification. *Applied Energy 254*, 113677.

Galanopoulos, G., E. Fytsilis, N. Yue, A. Broer, D. Milanoski, D. Zarouchas, and T. Loutas (2023). A data driven methodology for upscaling remaining useful life predictions: From single- to multi-stiffened composite panels. *Composites Part C: Open Access 11*, 100366.

Gerrard, R. and A. Tsanakas (2011). Failure probability under parameter uncertainty. *Risk Analysis 31*(5), 727–744.

Hersbach, H. (2000). Decomposition of the continuous ranked probability score for ensemble prediction systems. *Weather and Forecasting 15*(5), 559–570.

Khorasgani, H., G. Biswas, and S. Sankararaman (2016). Methodologies for system-level remaining useful life prediction. *Reliability Engineering & System Safety 154*, 8–18.

Kontogiannis, T., M. Salinas-Camus, and N. Eleftheroglou (2026). Himap: Hidden markov models for advanced prognostics. `https://github.com/GroupiSP/himap`.

Leontief, W. W. (1936). Quantitative input and output relations in the economic systems of the united states. *The Review of Economics and Statistics 18*(3), 105–125.

Loutas, T., A. Oikonomou, N. Eleftheroglou, F. Freeman, and D. Zarouchas (2022). Remaining useful life prognosis of aircraft brakes. *International Journal of Prognostics and Health Management 13*(1).

Palazuelos, A. R.-T. and E. L. Droguett (2021). System-level prognostics and health management: A graph convolutional network–based framework. *Proceedings of the Institution of Mechanical Engineers, Part O 235*(1), 120–135.

Rodrigues, L. R. (2018). Remaining useful life prediction for multiple-component systems based on a system-level performance indicator. *IEEE/ASME Transactions on Mechatronics 23*(1), 141–150.

Salinas-Camus, M., G. Galanopoulos, L. Amaral, E. I. L. Jull, and N. Eleftheroglou (2025). Robust prognostics of impacted composite structures using an adaptive hidden semi-markov model. *Structural Health Monitoring 0*(0), 14759217251368254.

Salinas-Camus, M., K. Goebel, and N. Eleftheroglou (2025). A comprehensive review and evaluation framework for data-driven prognostics: Uncertainty, robustness, interpretability, and feasibility. *Mechanical Systems and*

Signal Processing 237, 113015.

Shields, M. D., K. Teferra, A. Hapij, and R. P. Daddazio (2015). Refined stratified sampling for efficient monte carlo based uncertainty quantification. *Reliability Engineering & System Safety 142*, 310–325.

Tamssaouet, F., K. T. Nguyen, K. Medjaher, and M. Orchard (2021). A fresh new look for system-level prognostics: Handling multi-component interactions, mission profile impacts, and uncertainty quantification. *International Journal of Prognostics and Health Management 12*(2).

Tamssaouet, F., K. T. Nguyen, K. Medjaher, and M. E. Orchard (2023). System-level failure prognostics: Literature review and main challenges. *Proceedings of the Institution of Mechanical Engineers, Part O 237*(3), 524–545.

Tamssaouet, F., T. P. K. Nguyen, and K. Medjaher (2018). System-level prognostics based on inoperability input-output model. In *Annual conference of the prognostics and health management society 2018*, pp. 0.

Zio, E. (2025). Advances in reliability analysis and risk assessment for enhanced safety. *Journal of Reliability Science and Engineering 1*(1), 013002.

Zio, E. and N. Pedroni (2012). *Uncertainty characterization in risk analysis for decision-making practice*. FonCSI.